Structural and Multidisciplinary Optimization (2022) 65:4
https://doi.org/10.1007/s00158-021-03095-8

RESEARCH PAPER

An efficient Kriging-based framework for computationally demanding constrained structural optimization problems

Marcela A. Juliani[1] · **Wellison J. S. Gomes**[1]

Received: 3 March 2021 / Revised: 9 September 2021 / Accepted: 21 October 2021 / Published online: 14 December 2021

Abstract

A literature survey reveals that many structural optimization problems involve constraint functions that demand high computational effort. Therefore, optimization algorithms which are able to solve these problems with just a few evaluations of such functions become necessary, in order to avoid prohibitive computational costs. In this context, surrogate models have been employed to replace constraint functions whenever possible, which are much faster to be evaluated than the original functions. In the present paper, a global optimization framework based on the Kriging surrogate model is proposed to deal with structural problems that have expensive constraints. The framework consists of building a single Kriging model for all the constraints and, in each iteration of the optimization process, the metamodel is improved only in the regions of the design space that are promising to contain the optimal design. In this way, many constraints evaluations in regions of the domain that are not important for the optimization problem are avoided. To determine these regions, three search strategies are proposed: a local search, a global search, and a refinement step. This optimization procedure is applied in benchmark problems and the results show that the approach can lead to results close to the best found in the literature, with far fewer constraints evaluations. In addition, when problems with more complex structural models are considered, the computational times required by the framework are significantly shorter than those required by other methods from the literature, including another Kriging-based adaptative method.

Keywords Kriging · Structural optimization · Constraints · Surrogate models

1 Introduction

Structural optimization problems consist of finding a vector of design variables which minimizes an objective function and is subject to constraints (Spillers and MacBain 2009). Usually, the objective function is related to the weight or cost of the structure and the constraints correspond to design criteria, such as allowable stresses and displacements. Therefore, in these cases, evaluations of objective functions are simple to perform, while evaluations of constraints many times depend on the application of numerical models to represent the structural behavior.

Application of complex computational models, in an attempt to better represent the real behavior of structures, raised challenges in the field of structural optimization. Usually, such models lead to high computational efforts. For example, a single run of a structural analysis which takes into account the effects of material and geometric nonlinearities may easily demand several minutes of computational time, and many structural analyses are usually necessary to perform an optimization. Therefore, the optimization process must require as few as possible evaluations of the constraints to avoid prohibitive computational costs. If the problem presents many local minima, its solution becomes much more challenging, since application of global optimization procedures, such as metaheuristic optimizations algorithms (Holland 1975; Kennedy and Eberhart 1995; Yang 2005; Atashpaz-Gargari and Lucas 2007; Gonçalves et al. 2015), usually requires too many constraints evaluations.

In the literature, surrogate models, also known as metamodels, have been used to deal with problems that have expensive functions (Zhao et al. 2020; Chunna et al. 2020;

Responsible Editor: Matthew Gilbert

✉ Marcela A. Juliani
marcelajulianii@gmail.com

[1] Department of Civil Engineering, Center for Optimization and Reliability in Engineering (CORE), Federal University of Santa Catarina, Florianópolis, SC, Brazil

Kroetz et al. 2020). These metamodels correspond to an approximation of a function, in the entire design space, based on a small number of sample points. Thus, computationally expensive functions can be replaced by surrogate models which are much faster to be evaluated than the original functions (Forrester et al. 2008). In optimization, many authors proposed to include samples in an adaptive manner, according to metrics that try to identify regions which are important to improve the accuracy of the metamodel. However, the main focus of these studies is related to expensive objective functions, while a more limited number has addressed problems with constraints (Durantin et al. 2016; Qian et al. 2020; Zhang et al. 2018; Wu et al. 2018; Dong et al. 2020; Yang et al. 2020). In addition, studies that apply such approaches to structural problems are even more limited (Parr et al. 2012; Dong et al. 2016; Liu et al. 2017; Li et al. 2017; Dong et al. 2018; Shi et al. 2019).

Usually, these procedures adopt infill sampling criteria based on the concepts of expected improvement, probability of feasibility or model error, and some also apply space reduction strategies. Among the surrogate models applied for this purpose, Kriging (Krige 1951; Jones et al. 1998) can be highlighted due to the great flexibility of the model and the ability to estimate its uncertainty, which may facilitate the identification of important regions, under an optimization point of view.

Lee and Jung (2008) proposes the so-called constraint boundary sampling method (CBS) to build a metamodel that can accurately predict the optimal point while satisfying constraints, where sample points are sequentially located along the constraint boundary by using the mean squared error of the Kriging estimate. Meng et al. (2019) proposes another active learning method, which presents high performance in comparison with CBS. References Lee and Jung (2008) and Meng et al. (2019) both focus on reliability-based design optimization problems.

Dong et al. (2018) present, as an extension of a previous study (Dong et al. 2016), a global optimization approach based on space reduction, where two subspaces of the search space are created, one in the neighborhood of the best solution and the other in a region that covers promising samples, and a multi-start optimization is performed alternately on the subspaces and the global space, to explore the surrogate models and add new samples. Qian et al. (2020) presents an update approach of the Kriging surrogate model when applied to represent constraints. The approach is based on confidence intervals, and tries to assess if the feasibility status of the candidate design can be changed due to the interpolation uncertainty related to the Kriging predictor. In Dong et al. (2020) a discrete constrained optimization method based on Kriging is proposed, where a multi-start optimization is performed to find promising solutions in the continuous design range. After a projection of the solutions to the discrete space takes place, a k-nearest neighbors search strategy is used, in conjunction with the expected improvement criterion, to find supplementary samples.

Although the approaches found in the literature seem promising and have been continually discussed, they usually focus on specific types of optimization problems. Studies that employ surrogate models for the constraints and aim at more general structural optimization problems were not found by the authors of the present paper, and this is one of the main purposes of the method presented herein.

In this context, the present paper proposes a global optimization framework based on surrogate models, for structural problems with computationally expensive constraints. The approach consists of building a single Kriging model for all the constraints from a set of sample points and, in each iteration of the method, adding points to this set only in the regions of the domain that are promising to contain the global optimum. In this way, many unnecessary constraints evaluations are avoided. For this, three search strategies are performed during the optimization process, using the metamodel: a local search, which is based on the farthest apart subset concept and applies a metaheuristic optimization method to look for multiple local minima along the design space; a global search, which is also performed by using a metaheuristic optimization method in an attempt to find the global minima; and a refinement step, which aims to improve the best solution found so far using a gradient-based method. Seven optimization problems from the literature are evaluated, where different types of structures, design variables, objective functions and constraints are addressed.

It is noteworthy that the objective here is not necessarily to obtain the best result in comparison with the results presented in the literature, but rather to find feasible results close to the best, with far fewer constraints evaluations. This may significantly accelerate the solution of large structural optimization problems, leading to viable solutions to practical engineering problems. Moreover, as the objective functions of the problems defined here demand low computational effort, it is not advantageous to replace them by a surrogate model, since the time to determine the parameters of the metamodel could be longer than the time to evaluate the true functions.

The remainder of this paper is organized as follows: Sect. 2 presents the surrogate model considered herein; the proposed global optimization framework is described in Sect. 3; Sect. 4 presents the application of the proposed approach in numerical examples; conclusions about the performance and accuracy of the framework are drawn in Sect. 5.

2 Surrogate model

Surrogate model is a mathematical model constructed based on a limited data set from a computational or physical experiment. Thus, it is possible to use the surrogate model in order to predict the results assumed by the experiment, without performing it (Forrester et al. 2008). In the context of optimization, surrogate models can be used, for example, to replace objective and/or constraint functions, when these functions demand high computational efforts to be evaluated. The main idea is to obtain metamodels sufficiently accurate and with construction and evaluation time considerably shorter than the evaluations of the original functions.

Considering a sampling plan $\mathbf{X} = \left[\mathbf{x}^{(1)}, ..., \mathbf{x}^{(n)}\right]^T$ formed by n points of the m-dimensional design space. Each one of these points can be associated with a value of the function $f(\mathbf{x})$ to be replaced. In this way, one can calculate the responses vector $\mathbf{y} = \left[y^{(1)}, ..., y^{(n)}\right]^T$, where $y^{(i)} = f(\mathbf{x}^{(i)})$, with $i = 1, ..., n$. From these data, it is possible to fit a surrogate model and to obtain predictions $\hat{y}(\mathbf{x}) \approx f(\mathbf{x})$ at any point $\mathbf{x}$ from design space, via metamodel. There are several surrogate models that can be used for this purpose, and Kriging is adopted.

2.1 Kriging

Kriging models can be seen as the realization of a Gaussian process, understood as

$$G(\mathbf{x}) = \mu + Z(\mathbf{x}), \tag{1}$$

where μ is the deterministic part which gives an approximation of the response in the mean (global trend) and $Z(\mathbf{x})$ is a stationary Gaussian process with zero mean (Echard et al. 2011), which represents a local deviation from the model (local trend). $Z(\mathbf{x})$ can be obtained by using the correlation between the local position and its nearby observations (Chunna et al. 2020). The covariance between outputs of the Gaussian process Z is given by

$$\text{Cov}\left[Z\left(\mathbf{x}^{(i)}\right), Z\left(\mathbf{x}^{(j)}\right)\right] = \sigma^2 R\left(\mathbf{x}^{(i)}, \mathbf{x}^{(j)}\right), \tag{2}$$

where σ^2 is the process variance and $R\left(\mathbf{x}^{(i)}, \mathbf{x}^{(j)}\right)$ is the correlation function (or basis function) between points $\mathbf{x}^{(i)}$ and $\mathbf{x}^{(j)}$, with $i, j = 1, ..., n$ (Bichon 2008). The most commonly used correlation function is Gaussian (Eq. (3)), which is also used herein, where $\boldsymbol{\theta} = \left[\theta_1, ..., \theta_m\right]^T$ are the unknown parameters of the model.

$$R\left(\mathbf{x}^i, \mathbf{x}^j\right) = \exp\left[-\sum_{l=1}^{m} \theta_l \left|x_l^{(i)} - x_l^{(j)}\right|^2\right] \tag{3}$$

In Kriging, the unknown parameters $\boldsymbol{\theta}$ are usually found by using the Maximum Likelihood Estimate (MLE). More details of the procedure can be obtained in Forrester et al. (2008).

For given $\mathbf{X}$, $\mathbf{y}$ and $\boldsymbol{\theta}$, $\hat{\mu}$ and $\hat{\sigma}$ can be estimated by

$$\hat{\mu} = \frac{\mathbf{1}^T\mathbf{R}^{-1}\mathbf{y}}{\mathbf{1}^T\mathbf{R}^{-1}\mathbf{1}}, \quad \hat{\sigma}^2 = \frac{(\mathbf{y} - \mathbf{1}\hat{\mu})^T\mathbf{R}^{-1}(\mathbf{y} - \mathbf{1}\hat{\mu})}{n}, \tag{4}$$

where $\mathbf{R}$ is the correlation matrix of all the observed data and $\mathbf{1}$ is an $n \times 1$ column vector of ones (Forrester et al. 2008). Therefore, the resulting prediction function and the respective mean squared error (MSE) can be written as in Eqs. (5) and (6), respectively, where $\mathbf{r}$ is the vector of correlations between the observed data and the new prediction.

$$\hat{y}(\mathbf{x}) = \hat{\mu} + \mathbf{r}^T\mathbf{R}^{-1}(\mathbf{y} - \mathbf{1}\hat{\mu}) \tag{5}$$

$$s^2(\mathbf{x}) = \hat{\sigma}^2\left[1 - \mathbf{r}^T\mathbf{R}^{-1}\mathbf{r} + \frac{\left(1 - \mathbf{1}^T\mathbf{R}^{-1}\mathbf{r}\right)^2}{\mathbf{1}^T\mathbf{R}^{-1}\mathbf{1}}\right] \tag{6}$$

Figure 1 shows an example of a function prediction via Kriging, as well as the estimate of the prediction error.

3 Global optimization framework

The optimization problem addressed herein consists of finding the values of the design variables $\mathbf{x}$ that minimize the objective function $f(\mathbf{x})$, subject to inequality constraints $g_i(\mathbf{x}) \leq 0$ and to lower and upper bounds of each variable x_j, with $i = 1, ..., p$ and $j = 1, ..., m$, where p and m are the numbers of constraints and design variables (or dimension of

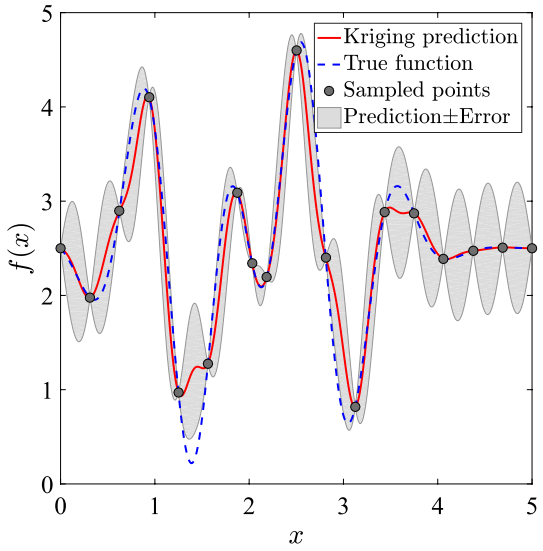

Fig. 1 Example of Kriging metamodel prediction

the design space), respectively. It is considered that objective functions are cheap to evaluate and that constraints require high computational effort, as previously discussed.

Since the surrogate model is used as an approximation of the constraints, based on sampled points, it is prudent to improve the accuracy of the metamodel during the optimization process, by inserting infill points (IPs) in regions of the design space that may contain the best design. In general, an optimization procedure based on metamodels can be summarized in the following main steps:

(1) Determine a sampling plan;
(2) Fit a surrogate model to the sampled points;
(3) Insert infill points in the sampling plan and go to the step 2. The procedure is performed until a stop criterion is reached.

The approaches adopted in the framework proposed herein are presented in the following sections, with some illustrations of the method when applied in the solution of the Toy problem, adapted from Gramacy et al. (2015). Equations (7), (8) and (9) present the objective function and the constraints of the Toy problem addressed herein. For a better understanding of the framework, Fig. 2 shows the flowchart of the optimization process. All codes are developed in MATLAB (MathWorks 2017) and the Kriging algorithm adopted herein is the one available in Forrester et al. (2008).

$$f(\mathbf{x}) = x_1 + x_2 \tag{7}$$

$$g_1(\mathbf{x}) = \frac{3}{2} - x_1 - 2x_2 - \frac{1}{2}\sin\left(4\pi\left(x_1^2 - 2x_2\right)\right) \tag{8}$$

$$g_2(\mathbf{x}) = x_1^2 + x_2^2 - \frac{3}{2} \tag{9}$$

3.1 Sampling plan

The sampling plan $\mathbf{X} = \left[\mathbf{x}^{(1)}, ..., \mathbf{x}^{(n)}\right]^T$ is generated in such a way that the points selected to compose the sample are the points most distant from each other in the design space, ensuring wide coverage of the search space. To do so, n_{samp} random points are generated uniformly in the design space. Among these points, the one closest to the center of the search space is selected and included in the sampling plan. The next selected point is defined as the farthest apart point from those selected previously. The selection proceeds by the criterion of the maximum Euclidean distance between the points, until the n points which define the initial sampling plan are obtained. The design space used in the framework is normalized, so that the lower and upper bounds correspond to 0 and 1, respectively. Thus, variables with different magnitudes have the same contribution to the distances. Figure 3 shows a sample generated by the proposed procedure for the Toy problem, with $n = 12$. Note that other procedures could be used to obtain similar initial sampling plans. For

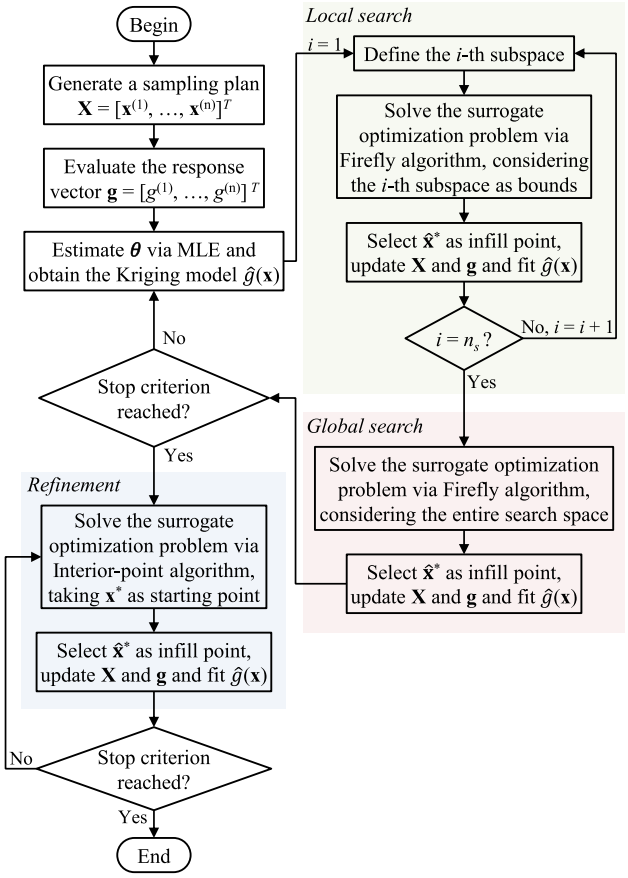

Fig. 2 Flowchart of the framework

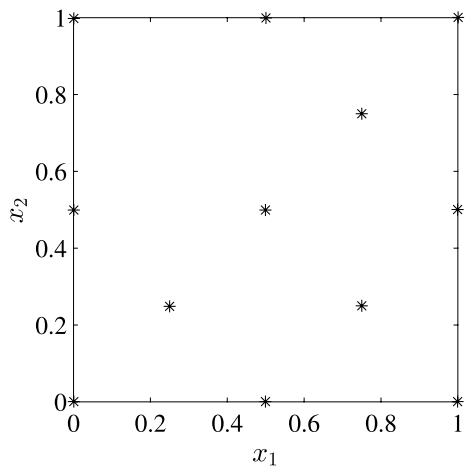

Fig. 3 Sampling plan of Toy problem

example, if Latin Hypercube Sampling (McKay et al. 1979) is employed, aiming at maximizing the minimum distance between points and with a sufficient number of improving iterations, it would lead to similar results.

3.2 Construction of the Kriging model

Here, a single surrogate model is created to represent all constraints of the problem, although different surrogates could be used to represent different constraints or groups of constraints. For this, it is necessary to evaluate the constraints at each sampled point, obtaining the response vector $\mathbf{g} = \left[g^{(1)}, ..., g^{(n)}\right]^T$, where $g^{(i)} = \max\left(\left[g_1(\mathbf{x}^{(i)}), ..., g_p(\mathbf{x}^{(i)})\right]\right)$, with $i = 1, ..., n$, and max is the operator that returns the maximum value among elements. So, the surrogate model is created based on the sampling plan $\mathbf{X}$ and the respective constraints values $\mathbf{g}$. The prediction obtained via the metamodel is denoted by $\hat{g}(\mathbf{x})$. To fit the parameters $\boldsymbol{\theta}$ of the basis function to the data set, the MLE is performed by Particle Swarm Optimization (PSO) (Kennedy and Eberhart 1995), which proved to be more accurate and faster than the genetic algorithm (GA) used in Forrester et al. (2008). Other metaheuristic optimization methods could also be employed, but the results obtained via PSO seemed to be good enough for the purposes of this paper.

3.3 Search strategies

Three search strategies used to select infill points are proposed herein. Note that the proposed framework differs from what has been found in the literature because it combines these three different strategies, which have complementary characteristics. As a result, the framework becomes more robust and sometimes faster than other procedures presented in the literature. To avoid further evaluations of the true time-consuming constraints, all of these strategies make use of a surrogate optimization problem, where the constraints are replaced by the prediction function $\hat{g}(\mathbf{x})$. The optimum points $\hat{\mathbf{x}}^*$ found in these optimizations are inserted as infill points in the sampling plan, even if they are classified as infeasible by the true functions. During the entire optimization process, the true constraints are evaluated only once, at each point of the sampling plan. The total number of evaluations of the constraints equals the size of the sampling plan. More details about the strategies are presented below.

3.3.1 Local search and global search

The local search is performed in order to look for multiple local minima over the design space, so that a number of promising regions may be explored. For this, n_s design subspaces are defined and, in each one of these subspaces, the surrogate optimization problem is solved via a metaheuristic optimization method. Firefly algorithm (FA) (Yang 2005) was chosen to be used herein due to its good performance in structural problems (Gandomi et al. 2011; Miguel and Fadel Miguel 2012; Miguel et al. 2015; Gebremedhen et al. 2020), although other global optimization methods could be employed. The best design $\hat{\mathbf{x}}^*$ found in each optimization subproblem is taken as an infill point. To generate the design subspaces, first a point in the sampling plan is randomly selected, defining $\mathbf{x}_s^1$. The next points $\mathbf{x}_s^i$, with $i = 2, ..., n_s$, are chosen based on the farthest apart subset concept, selecting the point from the sampling plan which is the farthest from the already selected points. The lower and upper bounds of the i-th design subspace, defined as $\mathbf{lb}_s^i$ and $\mathbf{ub}_s^i$, respectively, are given by

$$\begin{aligned} \mathbf{lb}_s^i &= \max\left(\left[\mathbf{lb}, \left(\mathbf{x}_s^i + \triangle\mathbf{lb}^i - \triangle\mathbf{ub}^i\right) - \frac{\mathbf{d}}{2}\right]\right) \\ \mathbf{ub}_s^i &= \min\left(\left[\mathbf{ub}, \left(\mathbf{x}_s^i + \triangle\mathbf{lb}^i - \triangle\mathbf{ub}^i\right) + \frac{\mathbf{d}}{2}\right]\right), \end{aligned} \tag{10}$$

where all vectors sizes are $m \times 1$ and each row is associated with a dimension of the design space: $\mathbf{lb}$ and $\mathbf{ub}$ are the lower and upper bounds of the problem, respectively, $\mathbf{d}$ represents the widths of the subspace and $\triangle\mathbf{lb}^i$ and $\triangle\mathbf{ub}^i$ are calculated by

$$\begin{aligned} \triangle\mathbf{lb}^i &= \max\left(\left[\mathbf{0}, \mathbf{lb} - \left(\mathbf{x}_s^i - \frac{\mathbf{d}}{2}\right)\right]\right) \\ \triangle\mathbf{ub}^i &= \max\left(\left[\mathbf{0}, \left(\mathbf{x}_s^i + \frac{\mathbf{d}}{2}\right) - \mathbf{ub}\right]\right). \end{aligned} \tag{11}$$

In addition, max and min are the operators that return the maximum and minimum value of a row, respectively. All subspaces have the same size, chosen as $\mathbf{d} = (\mathbf{ub} - \mathbf{lb})/(\mathbf{n_s^{1/m}})$, which result in some superpositions between them if the value of $\mathbf{d}$ is greater than half the range defined by $\mathbf{ub}$ and $\mathbf{lb}$, in any dimension of the problem. The boundaries given by Eqs. (10) and (11) tend to center the subspaces in their respective $\mathbf{x}_s^i$. However, when these points are close to the bounds, the subspace cannot be centered on them. The subspaces must be relocated so that the upper and lower bounds are not violated. Figure 4 shows two possible sets of subspaces generated from different $\mathbf{x}_s^1$. It should be noted that, given the random aspect of the selection of the first subspace point and due to the updating of the sampling plan throughout the process, the subspaces change with each iteration of the method, so that different regions of the domain are explored during the optimization process.

On the other hand, the global search is employed in an attempt to find the global minima. Here, the surrogate optimization problem is solved considering the entire design space. The optimum point $\hat{\mathbf{x}}^*$ found in the process is selected as an IP. The optimization is also performed by the Firefly algorithm (FA).

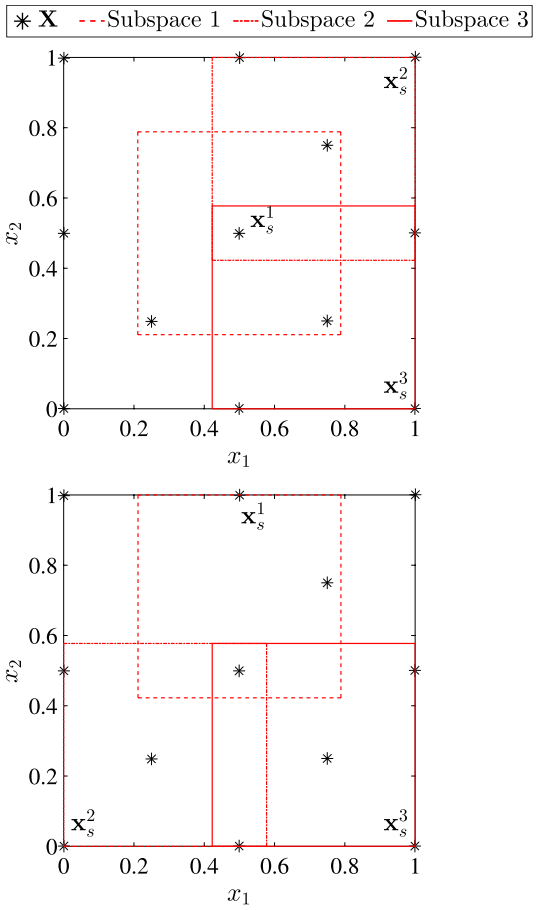

Fig. 4 Different subspaces obtained with the proposed formulation

The local and global searches are performed until a stop criteria is reached, which is defined in Sect. 3.4. Although the combination of these strategies has been found to be quite robust in finding the region of the global minimum, one more search strategy is needed to obtain more accurate results in this region, which corresponds to the refinement step.

3.3.2 Refinement

The refinement step corresponds to the solution of the surrogate optimization problem via a gradient-based method, starting from the best design $\mathbf{x}^*$ found so far. This point is chosen among those of the sampling plan which are feasible. The optimum point $\hat{\mathbf{x}}^*$ obtained in the refinement step is also taken as an IP. This procedure is performed several times, until a stop criterion is reached (Sect. 3.4). Similar strategies, when applied alone, can converge to a local minimum, as exemplified in Jones et al. (1998), in which a surrogate model is built for the objective function. However, in this framework, the design space is explored by the previous strategies, so that this step has only the objective of

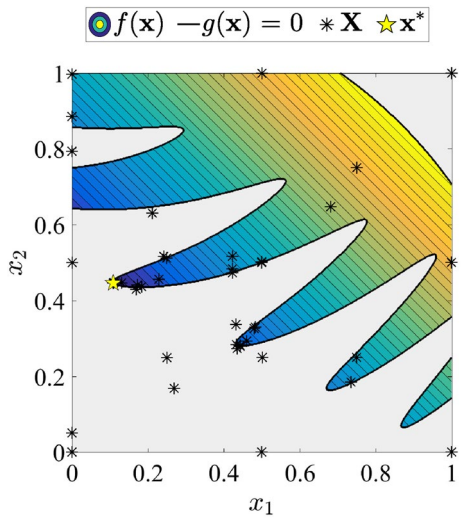

Fig. 5 Toy problem and the sampled points of the optimization process

improving the best result found in the region of the global minimum. The gradient-based method adopted herein is the Interior point (Coleman and Li 1996), which is an established method in the literature and is available in MATLAB.

Figure 5 illustrates the Toy problem and the points evaluated by $g(\mathbf{x})$ during the solution process, and Fig. 6 shows the behavior of $\hat{g}(\mathbf{x})$ in different stages of the framework. In the last iteration of the global search (Fig. 6b), it is possible to observe that most of the IPs were added in two regions of minimums and that in the refinement step (Fig. 6c), the IPs were added only in the region of the global minimum. In addition, the method was able to deal with the fact that, initially (Fig. 6a), the global optimum was considered to be unfeasible by the Kriging model.

3.4 Stopping criteria and optimal result

The stopping criterion adopted corresponds to the number it_{stall} of iterations in which the optimum result does not present improvements greater than a given tolerance f_{tol} between consecutive iterations, also attending to a minimum it_{min} and maximum it_{max} number of iterations. After the stopping criterion is achieved, the optimal design $\mathbf{x}^*$ is taken as the feasible point of the sampling plan that has the lowest value of the objective function.

4 Numerical examples

The proposed methodology is applied in the solution of seven structural optimization problems. In order to evaluate the performance of the framework, each example is run several times and some metrics such as best and mean results,

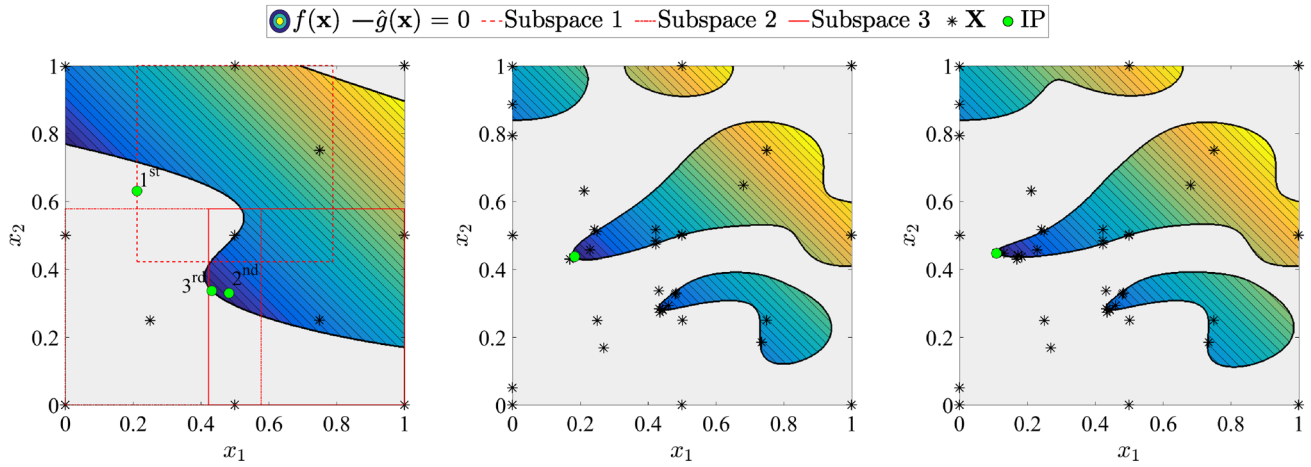

(a) Local search in the first iteration. **(b)** Global search in the last iteration. **(c)** End of the refinement step.

Fig. 6 Search strategies during the optimization process of Toy problem

standard deviation (Std) and mean number of constraint function evaluations (FE) are presented.

The numerical examples are divided in two sections: the first (Sect. 4.1) corresponds to the solution of benchmark examples, and the results of the framework are compared with the results of the literature; the second (Sect. 4.2) presents the solution of examples also taken from the literature, but with modifications in the structural model adopted. In this case, as no results were found in the literature for these examples, they are also solved by other methods from the literature for comparison purposes. The first method is the Firefly algorithm (FA) discussed in Sect. 3.3.1. The second is an adaptive metamodeling-based method described in Forrester et al. (2008), represented herein by KG-GA. In KG-GA, initially a Kriging model is constructed for the constraints, based on a Latin Hypercube sampling plan, and subsequently, the minimums found in successive solutions of the surrogate optimization problem via genetic algorithms are selected as infill points.

Although each one of these approaches has a different main purpose, the objective of these comparisons is to investigate if the proposed method is capable of providing similar results with fewer constraints evaluations, for the problems at hand.

The input data of the framework used in all examples, except when specified otherwise, are given by the following: $n_{samp} = 1 \cdot 10^6$; $n = \min([10m\ 150])$; $n_s = \min([2m\ 20])$; $it_{stall} = 2$, $f_{tol} = 0.1$, $it_{min} = 3$ and $it_{max} = 12$ for the first stop criterion, related to the global and local searches; $it_{stall} = \min([2m\ 30])$, $f_{tol} = 0.001, it_{min} = \min([10m\ 150])$ and $it_{max} = \min([20m\ 300])$ for the second stop criterion, related to the refinement step. In Sect. 4.1, each example is run 100 times, while the examples in Sect. 4.2 are run only 15 times due to the high computational effort of some of them. It is noteworthy that most of the parameters adopted herein are defined as proportional to the number of dimensions of the optimization problems. For example, the number of subspaces adopted corresponds to twice the number of design variables of the evaluated problem, since preliminary tests indicated that this value is sufficient to adequately cover the design space with subspaces. Such value is limited to 20, in order to avoid prohibitive computational effort in large problems. However, a more rigorous analysis of some of these parameters could be performed in future studies to try to further improve the proposed framework.

4.1 Benchmark problems

4.1.1 Tubular column

The first optimization problem corresponds to a tubular column, illustrated in Fig. 7, addressed by Hsu and Liu (2007), Gandomi et al. (2013) and Rao (2020), which has length $L = 250$ cm and is under a compressive load $P = 2500$ kgf. The material has a yield stress $\sigma_y = 500$ kgf/cm^2 and modulus of elasticity $E = 0.85 \cdot 10^6$ kgf/cm^2. The aim is to find the dimensions t and d that minimize the cost of the structure (Eq. (12)) and that meets the constraints of yield stress (Eq. (13)) and buckling stress (Eq. (14)). The lower and upper bounds are, in cm, $2 \leq d \leq 14$ and $0.2 \leq t \leq 0.8$. Table 1 shows the results obtained herein and some others available in the literature.

$$f(\mathbf{x}) = 9.82dt + 2d \tag{12}$$

$$g_1(\mathbf{x}) = \frac{P}{\pi dt\sigma_y} - 1 \leq 0 \tag{13}$$

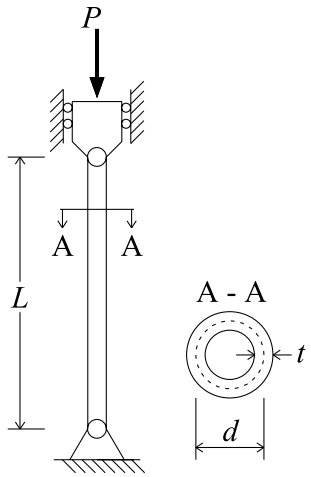

Fig. 7 Tubular column problem

Table 1 Optimal design and statistical results obtained by different methods for Tubular column problem

Design	CS (Gandomi et al. 2013)	Present study
d (cm)	5.45139	5.45285
t (cm)	0.29196	0.29194
g_1	− 0.0241	-2.12×10^{-4}
g_2	− 0.1095	-8.30×10^{-4}
Best	26.53217	26.53802
Mean	26.53504	26.59322
Std	0.00193	0.06226
FE	15000	67

$$g_2(\mathbf{x}) = \frac{8PL^2}{\pi^3 Edt\left(t^2 + d^2\right)} - 1 \leq 0 \tag{14}$$

4.1.2 I-beam

The second problem corresponds to a simply supported I-beam, studied by Wang (2003), Gandomi et al. (2013) and Cheng and Prayogo (2014). The problem consists of finding the dimensions of the cross section of the structure, which minimizes the vertical displacement and which meets the constraints of maximum cross-sectional area and of bending stress. Figure 8 shows the structure, where $L = 200$ cm, $P = 600$ kN and $Q = 50$ kN (both loads in the middle of the span), with modulus of elasticity equal to $2 \cdot 10^4$ kN/cm^2, maximum allowable bending stress of 6 kN/cm^2 and maximum cross-sectional area of 300 cm^2. The design space is, in cm, $10 \leq h \leq 80, 10 \leq b \leq 50, 0.9 \leq t_w \leq 5$ and $0.9 \leq t_f \leq 5$. Equation (15) corresponds to the objective function and Eqs. (16) and (17) define the constraints. Due to the order of magnitude of the $f(\mathbf{x})$, $f_{tol} = 0.001$ and $f_{tol} = 0.00001$ are

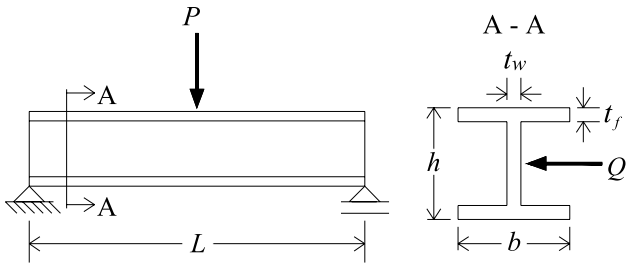

Fig. 8 I-beam problem

Table 2 Optimal design and statistical results obtained by different methods for I-beam problem

Design	CS (Gandomi et al. 2013)	SOS (Cheng and Prayogo 2014)	Present study
h (cm)	80.000000	80.00000	80.0000000
b (cm)	50.000000	50.00000	49.9999999
t_w (cm)	0.900000	0.90000	0.9000000
t_f (cm)	2.3216715	2.32179	2.3217905
g_1 (cm^2)	–	–	-1.71×10^{-4}
g_2 (kN/cm^2)	–	–	−1.57
Best (cm)	0.0130747	0.0130741	0.0130741
Mean (cm)	0.0132165	0.0130884	0.0132591
Std (cm)	0.0001345	0.00004	0.0003577
FE	5000	5000	122

adopted for the first and second stopping criteria, respectively, and the results achieved are shown in Table 2.

$$f(\mathbf{x}) = \frac{5000}{\frac{t_w(h-2t_f)^3}{12} + \frac{bt_f^3}{6} + 2t_f b\left(\frac{h-t_f}{2}\right)^2} \tag{15}$$

$$g_1(\mathbf{x}) = 2bt_f + t_w(h - 2t_f) - 300 \leq 0 \tag{16}$$

$$g_2(\mathbf{x}) = \frac{180000h}{t_w(h-2t_f)^3 + 2bt_f\left(4t_f^2 + 3h(h-2t_f)\right)} + \frac{15000b}{2t_f b^3 + (h-2t_f)t_w^3} - 6 \leq 0 \tag{17}$$

4.1.3 10-bar truss

The 10-bar truss problem shown in Fig. 9 is often used as a benchmark example (Wei et al. 2005; Gomes 2011; Wei et al. 2011; Kaveh and Zolghadr 2011; Miguel and Fadel Miguel 2012; Kaveh and Zolghadr 2012; Zuo et al. 2014; Kaveh and Zolghadr 2017; Tejani et al. 2016, 2018; Kumar et al. 2019). The problem consists in finding the

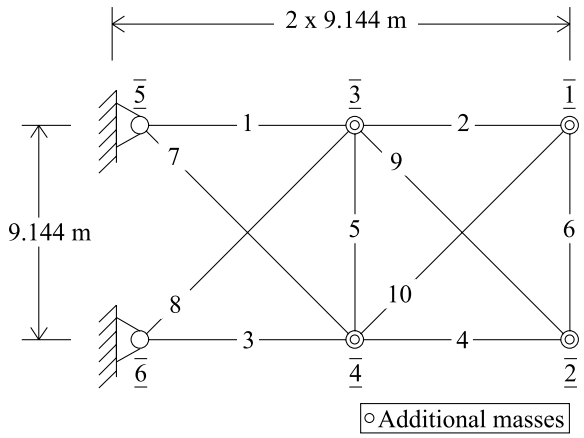

cross-sectional areas of the elements that minimize the mass of the structure, taking into account constraints based on the natural frequencies. Thus, 10 areas are considered as design variables, whose design space is $0.645\ \text{cm}^2 \leq A_i \leq 50\ \text{cm}^2$, with $i = 1, ..., 10$. The material has Young modulus equal to $6.98 \cdot 10^{10}$ Pa and density of 2770 kg/m^3. At all free nodes (nodes 1–4) non-structural masses of 454 kg are attached to the truss. The natural frequency constraints are $f_1 \geq 7$ Hz, $f_2 \geq 15$ Hz and $f_3 \geq 20$ Hz. Table 3 shows the results obtained by the framework using $it_{stall} = 4$ and $it_{min} = 6$ for the first stop criterion, due to the large number of variables.

Fig. 9 10-bar truss problem

Table 3 Optimal design and statistical results obtained by different methods for 10-bar truss problem

Design	PSO (Gomes 2011)	NHPGA (Wei et al. 2011)	Enhanced CSS (Kaveh and Zolghadr 2011)	SOS-ABF2 (Tejani et al. 2016)	ISOS (Tejani et al. 2018)	MSOS (Kumar et al. 2019)	Present study
A_1 (cm^2)	37.712	36.630	39.569	35.3013	35.2654	35.2834	34.9471
A_2 (cm^2)	9.959	13.043	16.740	14.8119	14.6803	14.4487	14.2342
A_3 (cm^2)	40.265	34.229	34.361	34.9522	34.4273	34.5268	33.7359
A_4 (cm^2)	16.788	15.289	12.994	14.9436	14.9605	14.6773	16.2597
A_5 (cm^2)	11.576	0.645	0.645	0.6450	0.6450	0.6450	0.6451
A_6 (cm^2)	3.955	4.8472	4.802	4.5828	4.5927	4.5878	4.9807
A_7 (cm^2)	25.308	22.140	26.182	23.5712	23.3417	23.5452	22.6882
A_8 (cm^2)	21.613	27.983	21.260	23.5602	23.8236	24.1081	24.1722
A_9 (cm^2)	11.576	15.034	11.766	11.9314	12.8497	12.7202	13.5150
A_{10} (cm^2)	11.186	10.216	11.392	13.0401	12.5321	12.4136	13.1714
f_1 (Hz)	7.000	7.0003	7.000	7.0003	7.0001	7.0000	7.0083
f_2 (Hz)	17.786	16.080	16.238	16.1997	16.1703	16.1666	16.1812
f_3 (Hz)	20.000	20.002	20.000	20.0022	20.0024	20.0012	20.0482
Best (kg)	537.98	535.14	529.25	524.8289	524.7341	524.5747	528.9017
Mean (kg)	540.89	542.1816	538.53	528.5501	530.0286	527.7970	537.9182
Std (kg)	6.84	1.722717	5.97	2.9827	3.4763	2.9121	6.7098
FE	2000	–	4000	4000	4000	4000	470

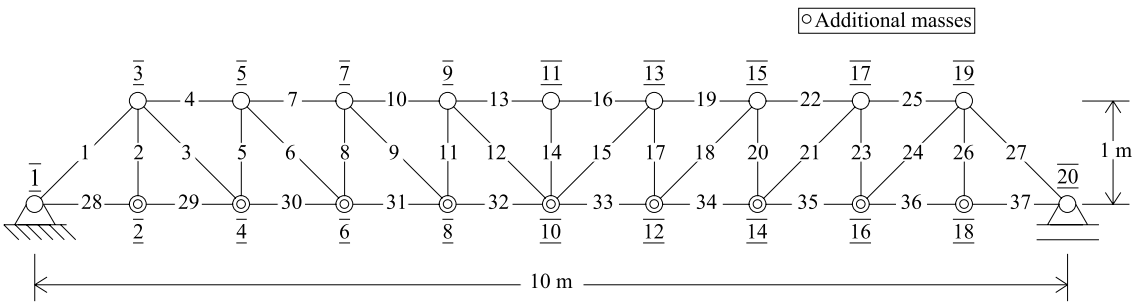

Fig. 10 37-bar truss problem

4.1.4 37-bar truss

The fourth problem select, as shown in Fig. 10, is a simply supported bridge studied by several authors (Wei et al. 2005; Gomes 2011; Wei et al. 2011; Kaveh and Zolghadr 2011; Miguel and Fadel Miguel 2012; Kaveh and Zolghadr 2017; Tejani et al. 2016, 2018; Kumar et al. 2019). Similar to the previous example, here the objective is to minimize the mass of the structure subjected to natural frequency constraints. However, in addition to the size variables (cross-sectional area), shape variables (vertical position of the nodes) are also adopted. Lower nodes are considered to be fixed and lower elements (bar 28 to 37) are assumed to have fixed cross-sections of 40 cm^2. Since symmetry of structure about its middle vertical plane is considered, the problem has 14 size variables, whose design space is 1 $cm^2 \leq A_i \leq 10$ cm^2, with $i = 1, ..., 14$, and 5 shape variables, whose design space is 0.1 m $\leq y_j \leq 3$ m, with $j = 3, 5, 7, 9, 11$. The material has Young modulus equal to $2.1 \cdot 10^{11}$ Pa and density of 7800 kg/m^3. In addition, non-structural masses equal to 10 kg are attached at each of the nodes on the lower chord. The natural frequency constraints are $f_1 \geq 20$ Hz, $f_2 \geq 40$ Hz and $f_3 \geq 60$ Hz. As in the previous problem, $it_{stall} = 4$ and $it_{min} = 6$ are used to the first stop criterion, due to the large number of variables, while the other parameters are kept as previously defined. Table 4 compares the results of the problem.

Table 4 Optimal design and statistical results obtained by different methods for 37-bar truss problem

Design	PSO (Gomes 2011)	NHPGA (Wei et al. 2011)	Enhanced CSS (Kaveh and Zolghadr 2011)	FA (Miguel and Fadel Miguel 2012)	TWO (Kaveh and Zolghadr 2017)	SOS-ABF2 (Tejani et al. 2016)	ISOS (Tejani et al. 2018)	MSOS (Kumar et al. 2019)	Present study
y_3,y_{19} (m)	0.9637	1.09693	1.0289	0.9392	1.0039	0.9413	0.9257	1.0111	0.9536
y_5,y_{17} (m)	1.3978	1.45558	1.3868	1.3270	1.3531	1.3393	1.3188	1.4030	1.3066
y_7,y_{15} (m)	1.5929	1.59539	1.5893	1.5063	1.5339	1.5434	1.4274	1.6095	1.4661
y_9,y_{13} (m)	1.8812	1.76551	1.6405	1.6086	1.6768	1.6744	1.5806	1.7610	1.5907
y_{11} (m)	2.0856	1.87413	1.6835	1.6679	1.7728	1.7571	1.6548	1.8513	1.6180
A_1,A_{27} (cm^2)	2.6797	2.62463	3.4484	2.9838	2.8892	2.9344	2.6549	2.9619	4.0651
A_2,A_{26} (cm^2)	1.1568	1	1.5045	1.1098	1.0949	1.0256	1.0383	1.0202	1.0000
A_3,A_{24} (cm^2)	2.3476	1.00176	1.0039	1.0091	1.0213	1.0095	1.0000	1.0000	1.0000
A_4,A_{25} (cm^2)	1.7182	2.07586	2.5533	2.5955	2.6776	2.5838	3.0083	2.3282	3.0694
A_5,A_{23} (cm^2)	1.2751	1.22071	1.0868	1.2610	1.1981	1.1569	1.0024	1.1719	1.0000
A_6,A_{21} (cm^2)	1.4819	1.48922	1.3382	1.1975	1.1387	1.2548	1.4499	1.2374	1.0001
A_7,A_{22} (cm^2)	4.6850	2.30847	3.1626	2.4264	2.6537	2.5104	3.1724	2.1430	2.3981
A_8,A_{20} (cm^2)	1.1246	1.43236	2.2664	1.3588	1.4171	1.4626	1.2661	1.5308	1.4774
A_9,A_{18} (cm^2)	2.1214	1.64678	1.2668	1.4771	1.3934	1.5245	1.4659	1.4839	1.4455
A_{10},A_{19} (cm^2)	3.8600	2.87072	1.7518	2.5648	2.7741	2.4586	2.9013	2.4001	2.9988
A_{11},A_{17} (cm^2)	2.9817	1.50405	2.7789	1.1295	1.2759	1.1888	1.1537	1.1678	1.0000
A_{12},A_{15} (cm^2)	1.2021	1.31328	1.4209	1.3199	1.2776	1.3765	1.3465	1.5085	1.2751
A_{13},A_{16} (cm^2)	1.2563	2.32277	1.0100	2.9217	2.1666	2.2341	2.6850	2.0768	2.5864
A_{14} (cm^2)	3.3276	1.04258	2.2919	1.0004	1.0099	1.0007	1.0000	1.0075	1.0000
f_1 (Hz)	20.0001	20.0819	20.0028	20.0024	20.0279	20.0052	20.0119	20.0017	20.0659
f_2 (Hz)	40.0003	40.0961	40.0155	40.0019	40.0146	40.0048	40.0964	40.0018	40.0390
f_3 (Hz)	60.0001	60.0321	61.2798	60.0043	60.0946	60.0077	60.0066	60.0164	60.0774
Best (kg)	377.20	363.032	362.38	360.05	360.27	359.9050	360.7432	360.3018	361.4900
Mean (kg)	381.2	369.7024	365.75	360.37	363.75	363.0816	363.3978	362.9610	364.3028
Std (kg)	4.26	2.353248	3.461	0.26	2.48	1.8304	1.5675	1.7265	2.4106
FE	12500	–	4000	5000	–	4000	4000	4000	571

4.1.5 Discussion of results

In all examples, the best and the mean values found by the proposed framework were close to those indicated in the literature, with differences less than 1.92% in relation to the best reference found. On the other hand, the number of constraints evaluations required by the framework was at least 85.73% lower than the number of evaluations employed in the literature. Throughout the runs, the framework tended to provide similar results, as indicated by the small standard deviations observed.

4.2 Problems with nonlinear structural analysis

For each example in this section, two constraint scenarios are considered: scenario 1 corresponds to that taken from the literature, and scenario 2 evaluates a structural model that takes into account material and/or geometric nonlinearities. In both scenarios, the structural analysis is performed using the MASTAN2 software (McGuire et al. 2014; Ziemian and McGuire 2007).

Here, the performance of the framework is also evaluated in relation to the computational time required in the execution of the algorithms. For all examples, a population of 10 individuals and 100 iterations are adopted to the Firefly algorithm as well as to the genetic algorithm of the adaptive metamodeling-based method. For both methods, the number of constraints evaluations is limited to 1000, due to the high computational effort of some examples. In addition, the number of points that define the initial sampling plan of KG-GA is the same of the framework proposed herein.

4.2.1 8-story frame

The example consists of finding the cross-sectional areas of the elements of a frame, which minimize its weight and which meets a displacement constraint. This example has been studied by some authors (Camp et al. 1998; Nanakorn and Meesomklin 2001; Kaveh and Hassani 2009; Schevenels et al. 2014), but among these only Kaveh and Hassani (2009) use continuous variables. Figure 11 shows the frame where the elements are categorized into 8 groups. The lateral displacement at the top of the frame must be less than 2 in (5.08 cm). The material has modulus of elasticity equal to $29 \cdot 10^3$ ksi (200 GPa) and density of $2.83 \cdot 10^{-4}$ kip/in^3 (76.8 kN/m^3). Kaveh and Hassani (2009) disregards the effects of axial internal forces, but here it is considered. The design space adopted is 5 in^2 (32.26 cm^2) $\leq A_i \leq$ 30 in^2 (193.55 cm^2), with $i = 1, ..., 8$, and the following empirical relationship between the cross-sectional area (A) and the moment of inertia (I) is applied (Kaveh and Hassani 2009):

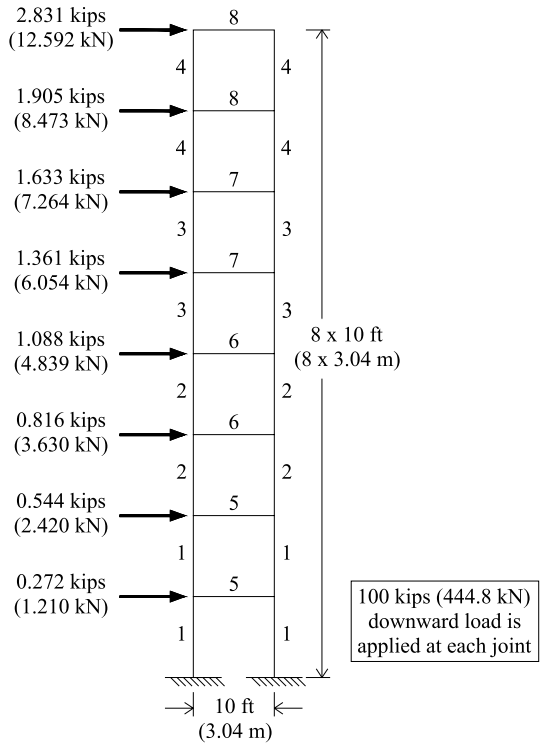

Fig. 11 8-story frame problem

$$I = \begin{cases} 4.592A^2 & 0 \leq A \leq 15 \\ 4.638A^2 & 15 \leq A \leq 44 \\ 256.229A - 2300 & 44 \leq A \leq 100 \end{cases} \quad (18)$$

While in the first scenario linear structural analyses are performed, geometric nonlinearities are considered in the second scenario. In this situation, the effects of deformations and displacements related to a load increase are included in the formulations of equilibrium equations. Table 5 shows the results obtained in both scenarios.

4.2.2 A model of Forth bridge

This example was previously evaluated by Gil and Andreu (2001) and Kaveh and Khayatazad (2013), although some modifications in relation to the number of design variables have been adopted herein, in order to reduce the computational time associated with the solution of the problem. The structure is shown in Fig. 12, where the configuration is symmetrical in relation to the middle vertical plane and the bars are categorized into three groups. The objective is to find the vertical position y_i of the nodes and the areas of the cross-sections A_j that minimize the weight of the structure, whose search space is -1.4 m $\leq y_i \leq$ 1.4 m and 25 cm^2 $\leq A_j \leq$ 100 cm^2, with $i = 2, ..., 11$ and $j = 1, ..., 3$. The

Table 5 Optimal design and statistical results obtained by different methods for 8-story frame problem

Design	Scenario 1: Linear analysis			Scenario 2: Nonlinear analysis		
	FA	KG-GA	Present study	FA	KG-GA	Present study
A_1 (cm^2)	70.6766	75.5689	75.5347	83.4353	87.2656	87.5108
A_2 (cm^2)	59.9734	57.4128	57.4709	74.0315	66.9592	67.1115
A_3 (cm^2)	39.5928	44.7122	44.7941	49.6489	51.4812	51.4044
A_4 (cm^2)	36.4819	33.7664	33.8470	38.3522	37.6773	37.4548
A_5 (cm^2)	68.8199	67.3760	67.0528	67.5734	73.9128	74.7263
A_6 (cm^2)	74.1360	69.2999	68.9192	80.4347	79.7076	79.0115
A_7 (cm^2)	65.8799	62.1599	62.2444	68.0218	70.7863	70.4444
A_8 (cm^2)	46.8470	42.5025	42.7438	56.7270	46.3451	46.3625
d (cm)	5.08	5.08	5.08	5.08	5.08	5.08
Best (N)	31,335.0410	31,106.8473	31,106.4025	35,763.2440	35,474.1097	35,473.2200
Mean (N)	33,533.3513	31,113.9644	31,108.1817	37,482.0362	35,483.4509	35,476.7786
Std (N)	1923.4103	4.0034	1.3345	1441.2233	5.3379	2.6689
FE	1000	1000	269	1000	1000	280
Time (min)	0.75	30.03	3.17	1.90	32.80	3.61

1 in = 2.54 cm; 1 in^2 = 6.4516 cm^2; 1 kip = 4448.22 N

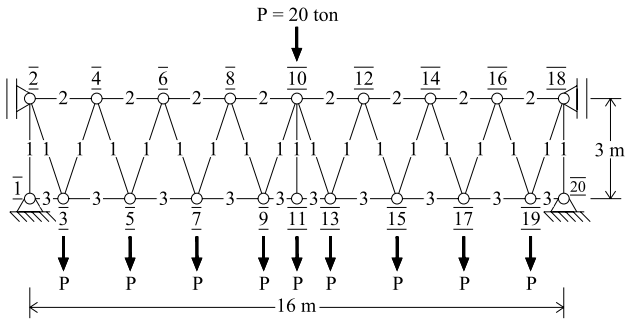

Fig. 12 A model of Forth bridge problem

modulus of elasticity of material is 2.1×10^8 kN/m^2 and the specific weight of material is 7.8 ton/m^3.

In the first scenario, the stress σ of the structural elements cannot exceed the maximum allowable stress $\sigma_{adm} = 25$ kN/cm^2. Therefore, the following constraint must be verified for each bar

$$g(\mathbf{x}) = \frac{\sigma(\mathbf{x})}{\sigma_{adm}} - 1 \leq 0. \tag{19}$$

In the second scenario, a single constraint is considered, given by

$$g(\mathbf{x}) = \frac{P}{P_{cr}(\mathbf{x})} - 1 \leq 0, \tag{20}$$

where P is the applied load and $P_{cr}(\mathbf{x})$ is the critical load, which is the maximum load value that the structure can handle before reaching failure. In this scenario, failure may occur due to buckling or yielding of one or more bars. In order to incorporate the possibility of buckling and yielding in the computation of the critical load, it is necessary to impose initial imperfections to each bar of the structure and to perform inelastic and geometrically nonlinear structural analyses. To do so, in this paper the initial imperfections are based on the first vibration mode of the structure, according to Eq. 21, and the materials are assumed to have elastic-perfectly plastic characteristics.

$$\mathbf{c} = \mathbf{c}_0 + 0.001\mathbf{u} \tag{21}$$

where

$\mathbf{c}$ = Vector of nodal coordinates after perturbation;

$\mathbf{c}_0$ = Vector of inicial nodal coordinates;

$\mathbf{u}$ = Vector of nodal displacements, according the vibration mode considered in the eigenvalue analysis.

In structural analysis, truss bars are modeled using several frame elements with moment releases at hinged connections. So elements that are connected to hinges are modeled as fixed-hinge frame element, while others are modeled as fixed-fixed elements. For more details about the model the readers are referred to Madah and Amir (2017) and Juliani et al. (2019), since the structural model adopted herein is very similar to the ones described in these references.

Table 6 shows the results, using $it_{stall} = 4$ and $it_{min} = 6$ to the first stop criterion, due to the large number of variables, while the other parameters are kept as previously defined.

4.2.3 120-bar dome truss

The 120-bar space truss was studied by several authors, with different variables, constraints, dimensions and loads (Soh and

Table 6 Optimal design and statistical results obtained by different methods for a model of Forth bridge problem

Design	Scenario 1: Linear analysis			Scenario 2: Nonlinear analysis		
	FA	KG-GA	Present study	FA	KG-GA	Present study
y_2,y_{18} (m)	0.1933	1.1890	0.7495	− 0.5901	0.1468	− 0.0428
y_3,y_{19} (m)	0.6219	0.3844	0.6346	1.0950	0.9888	1.0732
y_4,y_{16} (m)	0.0083	0.6445	0.1797	− 1.0205	− 0.7475	− 0.4594
y_5,y_{17} (m)	0.9399	1.0822	1.4000	0.2930	1.3999	1.4000
y_6,y_{14} (m)	− 0.8461	− 0.3977	− 1.4000	− 0.5256	− 1.0159	− 0.9085
y_7,y_{15} (m)	0.0423	0.9620	0.0497	− 0.1170	1.1200	0.6771
y_8,y_{12} (m)	− 0.6268	− 1.1110	− 1.4000	− 0.4673	− 1.1889	− 1.4000
y_9,y_{13} (m)	0.2558	1.0615	− 0.3173	− 0.2111	0.6084	0.2867
y_{10} (m)	− 0.1674	− 0.7230	− 0.8924	− 0.4277	− 1.2772	− 0.6163
y_{11} (m)	− 0.3654	1.0795	− 0.3031	− 0.1858	0.3192	0.4591
A_1 (cm^2)	27.0098	25.8654	25.0000	44.7308	44.1858	35.5438
A_2 (cm^2)	43.2129	38.1016	33.8999	59.8616	57.0754	51.9524
A_3 (cm^2)	51.2630	41.1818	31.6320	55.4994	58.2271	50.0472
max(g)	− 2×10^{-5}	− 0.0199	− 0.0053	− 0.0909	− 0.0109	− 0.0004
Best (N)	22,103.2770	19,163.1136	17,363.0220	30,288.0173	25,575.2898	22,830.0997
Mean (N)	27,190.8137	20,738.1630	18,282.4584	35,777.2050	27,904.5688	24,432.9214
Std (N)	2561.8445	759.1776	591.9464	4911.7407	1644.2231	1552.6187
FE	1000	1000	517	1000	1000	527
Time (min)	0.79	36.68	13.87	38.72	62.11	25.87

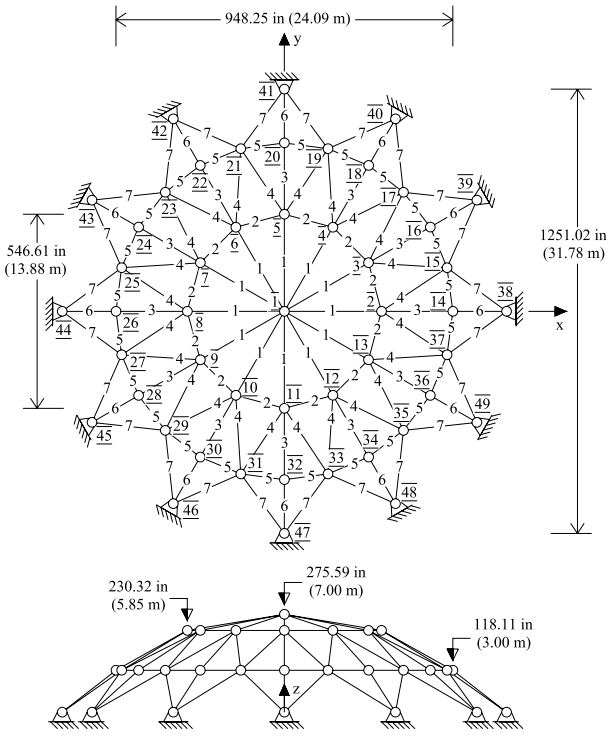

Fig. 13 120-bar dome truss problem

Yang 1996; Fallahian et al. 2009; Kaveh and Talatahari 2010; Kaveh and Khayatazad 2013; Kumar et al. 2019). Here, the configuration studied is the one presented by Fallahian et al. (2009) (Fig. 13).

In the first scenario, the allowable stresses σ_{adm} follow the requirements of the AISC ASD (1989) code, calculated by

$$\sigma_{adm} = \begin{cases} 0.6F_y & \text{for tensile stress} \\ F_{cr} & \text{for compression stress} \end{cases} \tag{22}$$

$$F_{cr} = \begin{cases} \left[\left(1 - \frac{\lambda_i^2}{2C_c^2}\right)F_y\right] / \left[\frac{5}{3} + \frac{3\lambda_i}{8C_c} - \frac{\lambda_i^3}{8C_c^3}\right] & \lambda_i < C_c \\ [10pt]12\pi^2 E/23\lambda_i^2 & \lambda_i \geq C_c \end{cases}. \tag{23}$$

In these equations, $C_c = \sqrt{2\pi^2 E/Fy}$ is the slenderness ratio dividing the elastic and inelastic buckling regions and $\lambda_i = kl_i/r_i$ is the member slenderness ratio, where F_y is the yield stress of steel, E is the modulus of elasticity, k is the effective length factor; l_i is the member length and $r_i = 0.4993A_i^{0.6777}$ is the radius of gyration, with $i = 1, ..., 120$. The vertical loads applied are − 13.49 kips (− 60 kN) at node 1, − 6.744 kips (− 30 kN) ate node 2 through 13 and − 2.248 kips (− 10 kN) at the rest of free nodes. The design variables are the cross-sectional areas of the bars, which are categorized into 7 groups, as shown in Fig. 13, whose design space adopted is 1.2 in^2 (7.74 cm^2) $\leq A_j \leq$ 10 in^2 (64.52 cm^2), with $j = 1, ..., 7$. The parameters F_y = 58 ksi (400 MPa), E = 30450 ksi (210 GPa), k = 1 are

Table 7 Optimal design and statistical results obtained by different methods for 120-bar dome truss problem

Design	Scenario 1: AISC ASD (1989)			Scenario 2: Nonlinear analysis		
	FA	KG-GA	Present study	FA	KG-GA	Present study
A_1 (cm^2)	24.8574	20.8419	20.2522	30.2186	31.7386	30.5116
A_2 (cm^2)	22.8871	15.4929	15.0638	28.0961	24.0658	23.5051
A_3 (cm^2)	19.8167	20.3961	20.0625	34.3148	32.0948	31.7025
A_4 (cm^2)	12.6845	12.7819	12.9329	18.4548	19.0458	19.6103
A_5 (cm^2)	11.3877	9.0509	7.7419	24.3741	7.7529	7.7419
A_6 (cm^2)	27.9980	18.8400	18.2296	27.5258	27.8909	27.8335
A_7 (cm^2)	15.1535	15.6503	15.2109	22.4735	22.5090	22.6703
max(g)	− 0.0008	− 0.0190	− 0.0099	− 0.0010	− 0.0010	− 0.0119
Best (kg)	8849.9240	7859.4448	7646.3781	12,506.0140	11,438.4958	11,398.3306
Mean (kg)	10,379.0716	8525.1939	8014.0666	13,708.6872	12,947.6762	11,766.6041
Std (kg)	923.7732	613.4274	290.4149	618.2429	1853.8914	421.2633
FE	1000	1000	325	1000	1000	328
Time (min)	0.79	29.24	5.97	146.83	114.19	35.64

1 in^2 = 6.4516 cm^2; 1 lb = 0.45359237 kg

adopted, and the material density is taken equal to 0.288 lb/in^3 (7971.81 kg/m^3).

The second scenario is similar to the previous example, where a single constraint based on a critical load is verified as a safety criterion. Table 7 shows the results obtained in both scenarios, where $it_{stall} = 4$ and $it_{min} = 6$ was adopted to the first stop criterion, as in the previous example.

4.2.4 Discussion of results

In all scenarios, the best results in terms of final objective function values were provided by the proposed framework, with means approximately 19% and 7% smaller than the ones provided by FA and KG-GA, respectively. In addition, the number of constraints evaluations required by the framework was at least 47.30% lower, reaching a 73.10% reduction in one case. It is noteworthy that the mean results achieved by the KG-GA with the same number of evaluations performed by the framework are on average 17.80% higher than those of the framework. This indicates a good performance of the proposed method, especially when dealing with complex problems, even in comparison with another metamodel-based method.

Regarding computational time, when simple problems are considered, the running time of Firefly is the lowest, although the standard deviation of its final responses is still very large. However, when nonlinear structural analyses are considered for larger structures, the framework surpasses both FA and KG-GA also in terms of running time. It should be noted the performance of the framework in scenario 2 of the 120-bar dome truss, where the times required by FA and KG-GA were above 2 h and almost 2 h, respectively, while better results were achieved by the framework in about half an hour. This emphasizes the fact that, due to its own computational demands, the framework should be applied only if the evaluations of the constraints are expensive enough.

5 Conclusion

In this paper, an optimization framework based on Kriging was presented to deal with structural problems that have expensive constraints. The main idea is to improve the accuracy of the surrogate model during the optimization process and only in promising regions of the design space. In order to identify these regions in a robust manner, the framework is composed of three search strategies: local search, global search, and refinement step. Seven examples from the literature were evaluated and the results were compared with those obtained by other optimization methods. It was found that the proposed framework achieved results close to the best presented in the literature, with far fewer constraints evaluations. Thus, the approach is found to be promising in reducing the computational effort associated with the solution of expensive constrained structural optimization problems, although as pointed out in other papers from the literature, there is a tendency of loss of efficiency when the dimensionality of the problems increases.

Acknowledgements The authors gratefully acknowledge the financial support from Scientific and Technological Research Support Foundation of Santa Catarina State and Coordination of Superior Level Staff Improvement (FAPESC/CAPES, public call nº 03/2017) and National Council for Scientific and Technological Development (CNPq, via Grant 302489/2017-7).

Declarations

Conflict of interest The authors declare that they have no conflict of interest.

Replication of results All the examples are implemented in MATLAB. The full datasets, as well as the source codes, can be available from the corresponding author upon request.

References

American Institute of Steel Construction (1989) Manual of steel construction: allowable stress design, 9th edn. American Institute of Steel Construction, Chicago

Atashpaz-Gargari E, Lucas C (2007) Imperialist competitive algorithm: an algorithm for optimization inspired by imperialistic competition. In: 2007 IEEE Congress on Evolutionary Computation, pp 4661–4667

Bichon BJ (2008) Efficient global reliability analysis for nonlinear implicit performance functions. AIAA J 46(10):2459–2468

Camp C, Pezeshk S, Cao G (1998) Optimized design of two-dimensional structures using a genetic algorithm. J Struct Eng 124(5):551

Cheng MY, Prayogo D (2014) Symbiotic organisms search: a new metaheuristic optimization algorithm. Comput Struct 139:98–112

Chunna L, Hai F, Chunlin G (2020) Development of an efficient global optimization method based on adaptive infilling for structure optimization. Struct Multidisc Optim 62:3383–3412

Coleman TF, Li Y (1996) An interior, trust region approach for nonlinear minimization subject to bounds. SIAM J Optim 6:418–445

Dong H, Song B, Dong Z, Wang P (2016) Multi-start space reduction (MSSR) surrogate-based global optimization method. Struct Multidisc Optim 54:907–926

Dong H, Song B, Dong Z, Wang P (2018) SCGOSR: surrogate-based constrained global optimization using space reduction. Appl Soft Comput 65:462–477

Dong H, Wang P, Song B, Zhang Y, An X (2020) Kriging-assisted discrete global optimization (KDGO) for black-box problems with costly objective and constraints. Appl Soft Comput J 94:106429

Durantin C, Marzat J, Balesdent M (2016) Analysis of multi-objective Kriging-based methods for constrained global optimization. Comput Optim Appl 63:903–926

Echard B, Gayton N, Lemaire M (2011) AK-MCS: an active learning reliability method combining kriging and Monte Carlo simulation. Struct Saf 33:145–154

Fallahian S, Hamidian D, Seyedpoor SM (2009) Optimal design of structures using the simultaneous perturbation stochastic approximation algorithm. Int J Comput Methods 6(2):1–16

Forrester AIJ, Sóbester A, Keane AJ (2008) Engineering design via surrogate modelling: a practical guide. Wiley, Chichester

Gandomi AH, Yang XS, Alavi AH (2011) Mixed variable structural optimization using Firefly algorithm. Comput Struct 89:2325–2336

Gandomi AH, Yang XS, Alavi AH (2013) Cuckoo search algorithm: a metaheuristic approach to solve structural optimization problems. Eng Comput 29:17–35

Gebremedhen HS, Woldemichael DE, Hashim FM (2020) A firefly algorithm based hybrid method for structural topology optimization. Adv Model Simul Eng Sci 7(44):1010

Gil L, Andreu A (2001) Shape and cross-section optimisation of a truss structure. Comput Struct 79:681–689

Gomes HM (2011) Truss optimization with dynamic constraints using a particle swarm algorithm. Expert Syst Appl 38:957–968

Gonçalves MS, Lopez RH, Miguel LFF (2015) Search group algorithm: a new metaheuristic method for the optimization of truss structures. Comput Struct 153:165–184

Gramacy RB, Gray GA, Digabel SL, Lee HKH, Ranjan P, Wellsk G, Wild SM (2015) Modeling an augmented lagrangian for black-box constrained optimization. Technometrics 58(1):1–11

Holland JH (1975) Adaptation in natural and artificial system. Univ. Michigan Press, Michigan

Hsu YL, Liu TC (2007) Developing a fuzzy proportional-derivative controller optimization engine for engineering design optimization problems. Eng Optim 39(6):679–700

Jones D, Schonlau M, Welch WJ (1998) Efficient global optimization of expensive black-box functions. J Glob Optim 13(4):455–492

Juliani MA, Milanez MO, Gomes WJS (2019) Structural optimization of trusses under elastic and inelastic buckling constraints. In: XL Ibero-Latin American Congress on Computational Methods in Engineering (CILAMCE)

Kaveh A, Hassani M (2009) Simultaneous analysis, design and optimization of structures using force method and ant colony algorithms. Asian J Civ Eng 10(4):381–396

Kaveh A, Khayatazad M (2013) Ray optimization for size and shape optimization of truss structures. Comput Struct 117:82–94

Kaveh A, Talatahari S (2010) Optimal design of skeletal structures via the charged system search algorithm. Struct Multidisc Optim 41:893–911

Kaveh A, Zolghadr A (2011) Shape and size optimization of truss structures with frequency constraints using enhanced charged system search algorithm. Asian J Civ Eng 12(4):487–509

Kaveh A, Zolghadr A (2012) Truss optimization with natural frequency constraints using a hybridized CSS-BBBC algorithm with trap recognition capability. Comput Struct 102–103:14–27

Kaveh A, Zolghadr A (2017) Truss shape and size optimization with frequency constraints using tug of war optimization. Asian J Civ Eng 18(2):311–333

Kennedy J, Eberhart R (1995) Particle swarm optimization. In: Proceedings of the 1995 IEEE-international conference on neural networks, pp 1942–1948

Krige DG (1951) A statistical approach to some basic mine valuation problems on the Witwatersrand. J S Afr Inst Miner Metall 52(6):119–139

Kroetz HM, Moustaphac M, Beck AT, Sudret B (2020) A two-level kriging-based approach with active learning for solving time-variant risk optimization problems. Reliab Eng Syst Saf 203:107033

Kumar S, Tejani GG, Mirjalili S (2019) Modified symbiotic organisms search for structural optimization. Eng Comput 35:1269–1296

Lee TH, Jung JJ (2008) A sampling technique enhancing accuracy and efficiency of metamodel-based RBDO: constraint boundary sampling. Comput Struct 86:1463–1476

Li Y, Wu Y, Zhao J, Chen L (2017) A kriging-based constrained global optimization algorithm for expensive black-box functions with infeasible initial points. J Glob Optim 67:343–366

Liu H, Xu S, Chen X, Wang X, Ma Q (2017) Constrained global optimization via a DIRECT-type constraint-handling technique and an adaptive metamodeling strategy. Struct Multidisc Optim 55:155–177

Madah H, Amir O (2017) Truss optimization with buckling considerations using geometrically nonlinear beam modeling. Comput Struct 192:233–247

MathWorks (2017) MATLAB: Primer

McGuire W, Gallagher RH, Ziemian RD (2014) Matrix structural analysis

McKay MD, Beckman RJ, Conover WJ (1979) A comparison of three methods for selecting values of input variables in the analysis of output from a computer code. Technometrics 21(2):239–345

Meng Z, Zhang D, Li G, Yu B (2019) An importance learning method for non-probabilistic reliability analysis and optimization. Struct Multidisc Optim 59:1255–1271

Miguel LFF, Fadel-Miguel LF (2012) Shape and size optimization of truss structures considering dynamic constraints through modern metaheuristic algorithms. Expert Syst Appl 39:9458–9467

Miguel LFF, Fadel Miguel LF, Lopez RH (2015) A firefly algorithm for the design of force and placement of friction dampers for control of man-induced vibrations in footbridges. Optim Eng 16:633–661

Nanakorn P, Meesomklin K (2001) An adaptive penalty function in genetic algorithms for structural design optimization. Comput. Struct 79:2527–2539

Parr JM, Keane AJ, Forrester AIJ, Holden CME (2012) Infill sampling criteria for surrogate-based optimization with constraint handling. Eng Optim 44(10):1147–1166

Qian J, Yi J, Cheng Y, Liu J, Zhou Q (2020) A sequential constraints updating approach for kriging surrogate model-assisted engineering optimization design problem. Eng Comput 36:993–1009

Rao SS (2020) Engineering optimization: theory and practice. Wiley, Chichester

Schevenels M, McGinn S, Rolvink A, Coenders J (2014) An optimality criteria based method for discrete design optimization taking into account buildability constraints. Struct Multidisc Optim 50:755–774

Shi R, Liu L, Long T, Wu Y, Tang Y (2019) Filter-based adaptive kriging method for black-box optimization problems with expensive objective and constraints. Comput Methods Appl Mech Eng 347:782–805

Soh CK, Yang J (1996) Fuzzy controlled genetic algorithm search for shape optimization. J Comput Civ Eng 10(2):143–150

Spillers WR, MacBain KM (2009) Structural optimization. Springer, New York

Tejani GG, Savsani VJ, Patel VK, Mirjalili S (2018) Truss optimization with natural frequency bounds using improved symbiotic organisms search. Knowl-Based Syst 143:162–178

Tejani GG, Savsanin VJ, Patel VK (2016) Adaptive symbiotic organisms search (SOS) algorithm for structural design optimization. J Comput Des Eng 3:226–249

Wang GG (2003) Adaptive response surface method using inherited Latin hypercube design points. J Mech Des 125(2):210–220

Wei L, Tang T, Xie X, Shen W (2011) Truss optimization on shape and sizing with frequency constraints based on parallel genetic algorithm. Struct Multidisc Optim 43:665–682

Wei L, Zhao M, Wu G, Meng G (2005) Truss optimization on shape and sizing with frequency constraints based on genetic algorithm. Comput Mech 35:361–368

Wu Y, Yin Q, Jie H, Wang B, Zhao J (2018) A RBF-based constrained global optimization algorithm for problems with computationally expensive objective and constraints. Struct Multidisc Optim 58:1633–1655

Yang X (2009) Firefly algorithms for multimodal optimization. In: Stochastic algorithms: foundations and applications, SAGA 2009, Lecture notes in Computer Sciences 5792, pp 169–178

Yang Z, Qiu H, Gao L, Cai X, Jiang C, Chen L (2020) Surrogate-assisted classification-collaboration differential evolution for expensive constrained optimization problems. Inf Sci 508:50–63

Zhang Y, Han ZH, Zhang KS (2018) Variable-fidelity expected improvement method for efficient global optimization of expensive functions. Struct Multidisc Optim 58:1431–1451

Zhao L, Wang P, Song B, Wang X, Dong H (2020) An efficient kriging modeling method for high-dimensional design problems based on maximal information coefficient. Struct Multidisc Optim 61:39–57

Ziemian RD, McGuire W (2007) Tutorial for MASTAN2: version 3.0. Wiley, Hoboken

Zuo W, Bai J, Li B (2014) A hybrid OC-GA approach for fast and global truss optimization with frequency constraints. Appl Soft Comput 14:528–535